Planar FET Oscillators Using Periodic Microstrip Patch Antennas

JOEL BIRKELAND, STUDENT MEMBER, IEEE, AND TATSUO ITOH, FELLOW, IEEE

Abstract — **Planar oscillators in which periodic microstrip antennas are integrated with FET negative resistance elements to form an integrated quasi-optical source are described. The antennas considered here are periodic microstrip patch arrays operated in the leaky-wave stopband. Because of the high *VSWR* in this case, this type of antenna may be used as both a resonant and a radiating element. Such circuits are suitable for use in millimeter-wave systems as well as at microwave frequencies. A design procedure is given and the performance of *X*-band prototype circuits is reported. Prototype circuits showed 9 dB isotropic conversion gain and 40 MHz tuning range at 9.5 GHz.**

I. Introduction

COMPONENTS formed by combining traditional circuit elements such as mixers, amplifiers, and oscillators with integral antennas find applications in systems where interconnections using transmission lines are inadequate. Such systems, where the interconnections are made by waves propagating in free space, are referred to as quasi-optical. Recently, many novel quasi-optical devices have been reported [1], [2]. Circuits in which an RF oscillator is integrated with an antenna to form a quasi-optical source find applications in the millimeter-wave range as local oscillators [3] and inter-injection-locked phase array elements [4]. At microwave frequencies they may be used in a variety of motion detection and process control schemes [5]. In the latter case they often take the form of Gunn diode cavity oscillators which are connected to a horn antenna. Such devices tend to be bulky and exhibit low efficiency.

In this paper we present a new type of integrated oscillator/antenna using a single microstrip leaky-wave structure as both the resonant and the radiating element. This resonant antenna is connected to a GaAs MESFET which acts as the negative resistance element in the oscillator circuit. This type of oscillator is similar in its operating principle to one reported using Gunn diodes and periodically notched dielectric image guide [6]. Our new circuit exhibits the high dc–RF conversion efficiency which is typical of FET oscillators. In addition, the planar circuit is simple and inexpensive to construct, occupies a small volume, and can conform to different surface profiles.

Manuscript received October 24, 1988; revised March 28, 1989. This work was supported by the U.S. Army Research Office under Contract DAAL03-88-K-005.

The authors are with the Department of Electrical and Computer Engineering, University of Texas at Austin, Austin, TX 78712

IEEE Log Number 8928845.

For certain types of linear periodic antennas, operation in the broadside region occurs in conjunction with very high *VSWR*; this is often referred to as the leaky-wave stopband. In conventional antenna applications this situation is avoided. However, in our present application we use this high *VSWR* to our advantage: the antenna functions as a frequency-selective element which reflects energy back to the negative resistance device, thereby sustaining oscillation. In this way, the antenna operates as both the resonant and the radiating element in our circuit.

Demonstration circuits in which this principle is applied at *X*-band frequencies have been constructed using commercially available packaged FET's integrated with microstrip antennas. The results show good directivity, high conversion gain, and a broad linear tuning range.

II. Oscillator Design

The oscillators that we describe here can be thought of as consisting of two parts: the negative resistance element, which supplies energy to the circuit, and the resonant element, which provides the frequency selection. The negative resistance element consists of an FET with the gate and source terminated in the proper way, and the resonant element consists of the leaky-wave antenna.

The oscillation condition for the circuit is given by

$$G_d + G_r = 0 \tag{1a}$$

$$B_d + B_r = 0 \tag{1b}$$

where G_d and B_d represent the conductance and susceptance of the negative resistance device, and G_r and B_r represent the conductance and susceptance of the resonant element. An alternative which is equivalent to the above is [7]

$$\Gamma_r \times \Gamma_d = 1 \tag{2}$$

where Γ_d and Γ_r represent the one-port reflection coefficients of the device and resonator, respectively. This last expression is quite useful when dealing with multiply resonant structures such as the microstrip arrays described in this paper, since with these structures it is possible for the oscillation condition to be satisfied at a number of different frequencies. In this case the product is plotted on the Smith chart as a function of frequency, and wherever the curve nears the point $R = \infty$, $jX = 0$, a possible oscillation is indicated. Using this information, the circuit can be

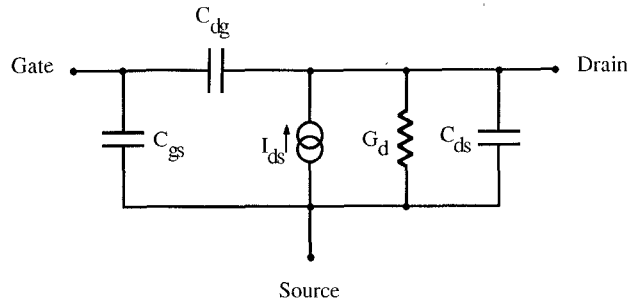

Fig. 1. A simplified small-signal equivalent circuit for the MESFET.

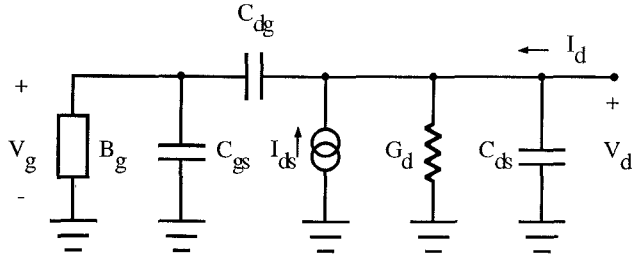

Fig. 2. A one-port circuit formed from the equivalent circuit of Fig. 1 by grounding the source and terminating the gate in a reactive load.

modified until oscillation is indicated at only the desired frequency.

As mentioned above, the device used in our design is a GaAs MESFET. By properly terminating the gate and the drain of the MESFET, we may regard it as a one-port negative-resistance device by looking into the drain.

Although the MESFET is necessarily a nonlinear device, many of the features of our circuit can be explained by using a linear model. A simple circuit model for the MESFET is shown in Fig. 1. If we operate in the common-source configuration and terminate the gate in reactance B_g, we arrive at the circuit of Fig. 2. Inserting the expressions

$$V_g = \frac{C_{dg}}{B_g + C_{gs}} V_d \qquad I_{ds} = g_m V_g$$

into the current equation at the drain node gives the following expression for the drain admittance of the device:

$$Y_d = \frac{I_d}{V_d} = \frac{-g_m}{B_g + C_{gs}} + j\omega \left[C_{dg} \left(\frac{B_g + C_{gs} - 1}{B_g + C_{gs}} \right) + C_{ds} \right].$$

Note that, depending on the value of B_g, the drain admittance may contain a negative real part. In addition, since the MESFET has a Schottky barrier type gate, the value of C_{gs} may be varied by changing the dc bias applied to the gate. Since this will affect both the magnitude and the phase of the drain admittance, the output power and the operating frequency may be adjusted in this way. In practice, an additional series feedback element may be added to the source to enhance the instability as well as to provide for dc bias connections.

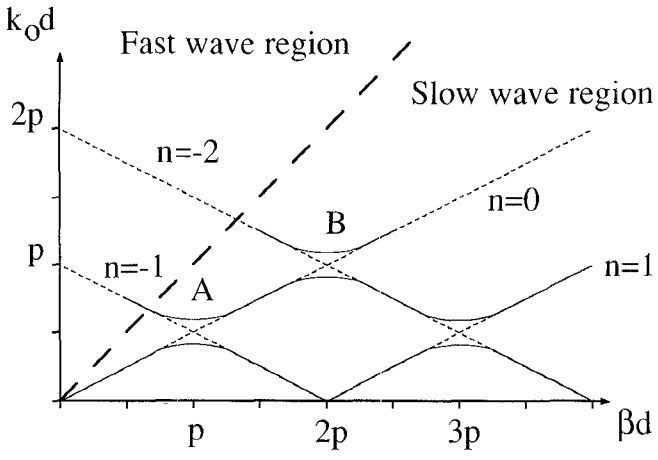

Fig. 3. The $k_0 d - \beta d$ diagram.

III. Periodic Structures

Although the microstrip leaky-wave structures used in our circuits are not strictly periodic, much insight into their operation can be gained by examining structures which are axially periodic, that is, structures which are invariant to an axial translation of distance d. For such a structure, the fields possess the following property [8]:

$$E(x, y, z + d) = e^{jk_{z0}d} E(x, y, z).$$

In this case, the fields may be expressed as the sum of spatial harmonics in the following way:

$$E(x, y, z) = \sum_{n=-\infty}^{n=\infty} a_n(x, y) e^{jk_{zn}z}$$

where k_{zn} are the spatial harmonic propagation constants,

$$k_{zn} = k_{z0} + \frac{2n\pi}{d}$$

and a_n are the spatial harmonic amplitudes. The dispersion curves may be plotted on a $k_0 d - \beta d$ diagram for a graphical interpretation.

For waves propagating in a basically slow guiding structure with an infinitesimal periodic perturbation, the $k_0 d - \beta d$ appears as shown in Fig. 3. The area of the diagram where $k_0 d > \beta d$ is called the fast wave region, where radiation from an open guiding structure may occur; the region where $k_0 d < \beta d$ is called the slow wave region. At the points where the curves representing the forward traveling and backward traveling waves cross, mode coupling occurs, creating stopbands. In the stopband regions, the coupling to the backward space harmonic creates high *VSWR* on the structure.

As the frequency is increased from low values, the first stopband encountered is at point A, where the β_0 and $-\beta_{-1}$ space harmonics are coupled. This is the so-called surface wave stopband since it occurs in the slow wave region of the $k_0 d - \beta d$ diagram. The next stopband is encountered at point B, and is due to the coupling between the β_0 and $-\beta_{-2}$ space harmonics. At the same time, the $-\beta_{-1}$ space harmonic is in the fast wave region and radiates in the broadside direction. This is the "leaky-

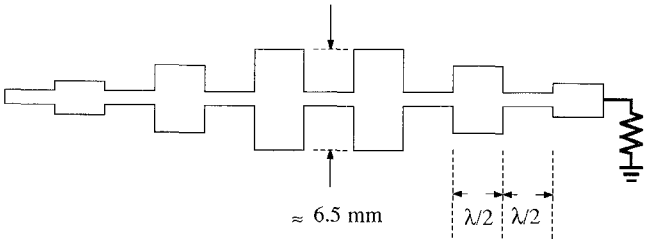

Fig. 4. Microstrip patch linear array: $\epsilon_r = 10.2$; $h = 0.635$ mm

wave" stopband, and it is in this region that we are interested in operating.

The preceding discussion involved only the general form of the dispersion curves in the limit of an infinitesimal perturbation. In practice, some of the space harmonics and stopbands may be missing due to additional symmetry of the structure. In addition, the presence of higher order modes is not taken into account.

The particular type of periodic antenna used in our project is a microstrip patch linear array consisting of varying width patch elements of approximate length $\lambda_g/2$ separated by sections of 50 Ω line of length $\lambda_g/2$, as shown in Fig. 4. The widths of the patch elements increase from the ends of the array to a maximum value in the center. The structure is terminated in a 50 Ω resistor. For this structure there occur parasitic elements due to the step changes in width at the junctions, which can be considered the periodic perturbations on the guiding structure. The radiation from this sort of discontinuity can be considered to arise from an equivalent magnetic current sheet in the transverse plane from the end of the patch element to ground. The radiated E field will therefore be polarized along the axis of the antenna.

IV. Circuit Design

In this section we discuss the design procedure for the oscillator in two parts: the active portion of the circuit and the antenna. All circuit design was performed using Touchstone from EEsof of Westlake Village, CA.

The first step in the design of the active portion of the circuit is the selection of the transistor. In our case the device used was the NEC 71083 ceramic packaged FET. This device is chosen since it exhibits a stability factor greater than the one at the design frequency of 10 GHz, indicating the potential for oscillation. Values of the S parameters supplied by the manufacturer are used in the remainder of the design steps.

Once the device is specified, the next step consists of plotting on the Smith chart its input stability circles in the common-source configuration. In this way we are able to determine the correct admittance to present to the gate of the device to ensure that the corresponding admittance at the drain port has a negative real part. Rather than simply connecting the source of the FET to ground, it is terminated in a quarter-wave open circuit line to facilitate the connection of dc bias. When the correct gate admittance is determined, the remainder of the design may be carried

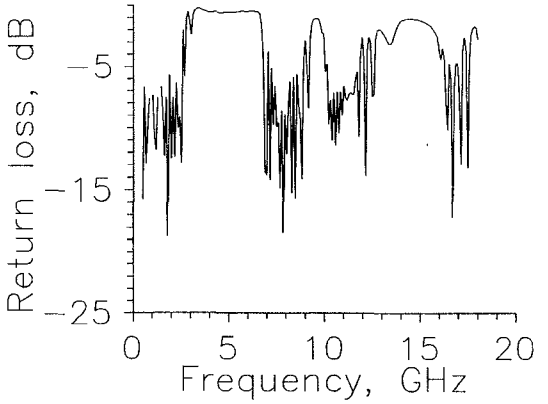

Fig. 5. Measured return loss for a microstrip patch array.

out from the point of view that the FET is now operating as a one-port negative-resistance element looking into the drain. More will be said about the gate circuit later.

In the design of the microstrip antenna, one must consider its performance as a resonator, and also its radiative properties. From the point of view of its resonant properties, we desire a high $VSWR$ at the oscillation frequency which drops off sharply as the frequency increases or decreases. For the antenna, we desire a highly directive beam of radiated energy. Fortunately, the two properties are closely related. The structure performs better in both respects as the length is increased, and as the energy is more evenly distributed along it.

The following empirical approach was used. The procedure begins with an analysis of a candidate microstrip structure using Touchstone, to determine its resonant properties, including stopband width and attenuation level. Once satisfactory performance is achieved on the computer, a prototype is constructed and its performance characteristics are measured using the network analyzer. Finally, a radiation pattern measurement is made.

After several trials, the following procedure was developed, which yielded structures that showed good all around performance. The centermost patch element was designed as an optimal single patch radiator, using the design rules given in [9]. Subsequent patch widths were decreased towards the ends of the array in a linear fashion. The length, and hence the number of elements, were chosen as a trade-off between stopband width and antenna length.

A plot of measured return loss for one of the antennas is shown in Fig. 5. From this we can see the broad surface wave stopband between 3 and 6 GHz, and the more narrow leaky wave stopband due to the microstrip discontinuities at about 9.7 GHz. Higher order stopbands are visible at higher frequencies.

The connection between the active portion of the circuit and the antenna was made using a microstrip line whose length was chosen to satisfy the conditions. Since the conditions listed in (1) are for the free running state, the following "start-up" conditions are used [10]:

$$G_d \approx -3G_r$$
$$B_d = -B_r.$$

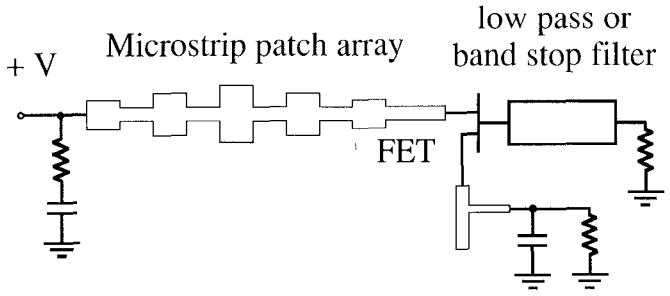

Fig. 6. Schematic view of oscillator circuit.

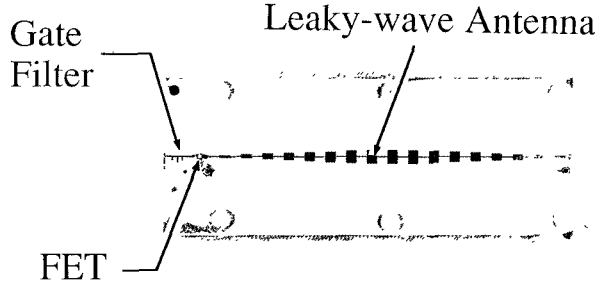

Fig 7. Photograph of oscillator circuit.

It was mentioned previously that for a multiply resonant circuit, the oscillation condition may be potentially satisfied at a number of frequencies. More specifically, this means that the relations

$$G_d > -G_r$$

$$B_d = -B_r$$

are satisfied. This is true for the leaky wave antenna described here due to the surface wave stopband at $f_0/2$. This becomes evident when the product in (2) is plotted on the Smith chart as a function of frequency. In order to prevent oscillation at this lower frequency, it becomes necessary to design the gate terminating network so as to present the correct admittance at f_0 and also to appear as a resistive termination at $f_0/2$. This requirement may be fulfilled by a low-pass filter with a cutoff between f_0 and $f_0/2$, or a bandstop filter centered at f_0.

A circuit diagram showing the final configuration is shown in Fig. 6. The supply of dc power to the FET is by means of the self-bias configuration, thereby allowing the use of a single positive supply. In practice, it was noted that the configuration of the termination resistor and bias network had little effect on the performance of the circuit.

V. Experimental Results

Three X-band prototype circuits were constructed on Rogers 6010.2 Duroid with a relative dielectric constant of 10.2 and thickness of 0.635 mm. Two circuits had 17-element antennas and one had a 12-element antenna. The 12-element circuit and one of the 17-element circuits used bandstop filters on the gate; the remaining circuit used a more compact low-pass filter. A photograph of this last circuit appears in Fig. 7.

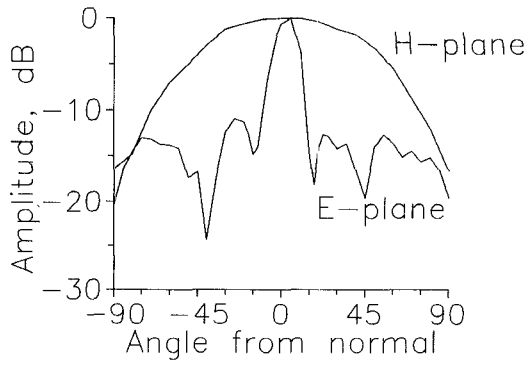

Fig. 8. Radiation patterns for circuit with 12-element antenna.

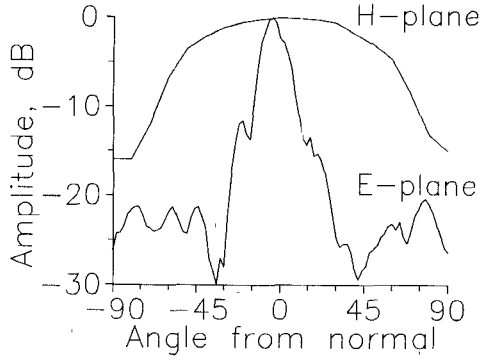

Fig. 9. Radiation patterns for circuit with 17-element antenna (circuit shown in Fig. 7).

Despite the fact that the design was performed using only small-signal models, all of the circuits oscillated within 5 percent of the design frequency, in the vicinity of 10 GHz. Only minor tuning, consisting of trimming the source open circuit stub, was required for alignment of the circuits. Radiation patterns for two of the circuits are shown in Figs. 8 and 9.

As a means of characterizing the performance of quasi-optical sources, we define the isotropic conversion gain of the devices as the ratio of received power in a particular direction to that due to a hypothetical isotropic source radiating with 100 percent dc–RF conversion efficiency. This definition follows a similar one for isotropic conversion loss given by Stephan and Itoh [11]. The effective radiated power (ERP) is computed by multiplying the dc input power by the isotropic conversion gain.

Isotropic conversion gain is measured by comparing the far-field intensity of the source with that of a standard gain horn driven with a known signal. For the circuit shown in Fig. 6, the isotropic conversion gain was measured at 9 dB in the broadside direction. In Fig. 10 we show the tuning range and output power variation for this same oscillator as we vary V_{gs} while holding V_{ds} constant. From this figure we can see the broad linear tuning range accompanied by only a small variation in output power.

VI. Conclusions

The quasi-optical planar oscillators described here may be considered to be the planar version of the cavity oscillator/horn antenna. The planar sources feature higher effi-

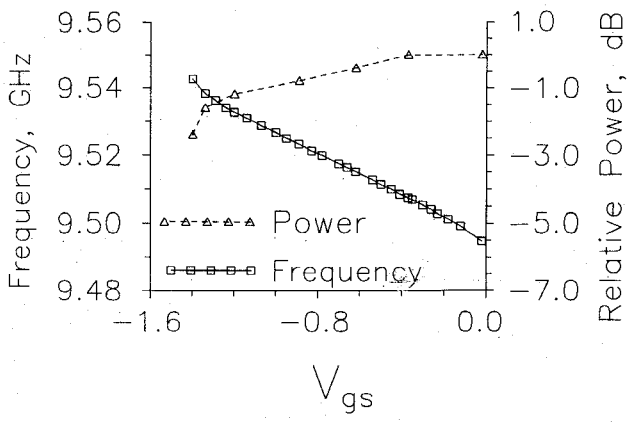

Fig. 10. Oscillation frequency and relative output power for the circuit shown in Fig. 7 as a function of gate-to-source voltage.

ciency and simpler construction than their waveguide counterparts and occupy a smaller volume. The planar structures also offer the possibility of conformability to different surface profiles. The X-band prototype circuits described in this report may be scaled for operation at higher frequencies.

Acknowledgment

The authors would like to thank Dr. D. P. Neikirk and the Microelectronics Research Center of the University of Texas at Austin for providing the equipment used for circuit fabrication, and also S. Wentworth and P. Cheung for their help in fabricating the circuits.

References

[1] V. D. Hwang, T. Uwano, and T. Itoh, "Quasi-optical integrated antenna and receiver front end," *IEEE Trans. Microwave Theory Tech.*, vol. 36, pp. 80–85, 1988.

[2] S. Nam, T. Uwano, and T. Itoh, "Microstrip-fed planar frequency-multiplying space combiner," *IEEE Trans. Microwave Theory Tech.*, vol. MTT-35, pp. 1271–1276, 1987.

[3] N.-L. Wang and S. E. Schwartz, "Planar oscillators for monolithic integration," *Int. J. Infrared and Millimeter Waves*, vol. 3, pp. 771–782, 1982.

[4] N. Camilleri and B. Bayraktaroglu, "Monolithic millimeter wave IMPATT oscillator and active antenna," in *1988 IEEE MTT-S Int. Microwave Symp. Dig.* (New York), pp. 955–958.

[5] *Microwave Sensing Modules and Sources*, publication no. 50050200, Alpha Industries, Inc., Semiconductor Division, Woburn, MA, 1987.

[6] B.-S. Song and T. Itoh, "Distributed Bragg reflection dielectric waveguide oscillators.," *IEEE Trans. Microwave Theory Tech.*, vol. MTT-27, pp. 1019–1022, Dec. 1979.

[7] G. D. Vendelin, *Design of Amplifiers and Oscillators by the S-Parameter Method*. New York: Wiley, 1982.

[8] R. E. Collin and F. J. Zucker, *Antenna Theory*. New York: Wiley, 1969, pt. II, ch. 19.

[9] I. J. Bahl and P. Bhartia, *Microstrip Antennas*. Dedham, MA: Artech House, 1980, ch. 2.

[10] G. Gonzales, *Microwave Transistor Amplifiers: Analysis and Design*. Englewood Cliffs, N.J.: Prentice-Hall, 1984, ch. 5.

[11] K. D. Stephan and T. Itoh, "A planar quasi-optical subharmonically pumped mixer characterized by isotropic conversion loss," *IEEE Trans. Microwave Theory Tech.*, vol. MTT-32, pp. 97–102, Jan. 1984.

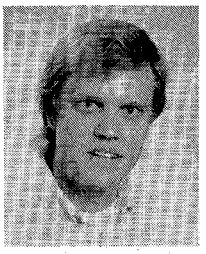

Joel Birkeland (S'87) received the B.S. degree in physics from Oregon State University in 1982 and the M.S.E. in electrical engineering from Arizona State University in 1985.

From February 1985 to August 1987 he was employed at M/A-COM Active Assemblies Division in Tempe, AZ, where he worked on low-noise hybrid microwave amplifiers. In September 1987 he entered the Ph.D. program in electrical engineering at The University of Texas at Austin on a University Fellowship. He was the recipient of an MTT-S fellowship for 1989.

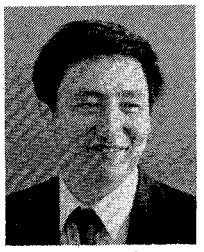

Tatsuo Itoh (S'69–M'69–SM'74–F'82) received the Ph.D. degree in electrical engineering from the University of Illinois, Urbana, in 1969.

From September 1966 to April 1976, he was with the Electrical Engineering Department, University of Illinois. From April 1976 to August 1977, he was a Senior Research Engineer in the Radio Physics Laboratory, SRI International, Menlo Park, CA. From August 1977 to June 1978, he was an Associate Professor at the University of Kentucky, Lexington. In July 1978, he joined the faculty at the University of Texas at Austin, where he is now a Professor of Electrical Engineering and Director of the Electrical Engineering Research Laboratory. During the summer of 1979, he was a guest researcher at AEG-Telefunken, Ulm, West Germany. Since September 1983, he has held the Hayden Head Centennial Professorship of Engineering at the University of Texas. In September 1984, he was appointed Associate Chairman for Research and Planning of the Electrical and Computer Engineering Department. He also holds an Honorary Visiting Professorship at the Nanjing Institute of Technology, China.

Dr. Itoh is a member of Sigma Xi and of the Institute of Electronics and Communication Engineers of Japan. He is a member of Commission B and Chairman of Commission D of USNC/URSI. He served as the Editor of the IEEE TRANSACTIONS ON MICROWAVE THEORY AND TECHNIQUES 1983–1985. He serves on the Administrative Committee of the IEEE Microwave Theory and Techniques Society. Dr. Itoh is a Professional Engineer registered in the state of Texas.